

REPORT DOCUMENTATION PAGE

Form Approved
OMB No. 0704-0188

Public reporting burden for this collection of information is estimated to average 1 hour per response, including the time for reviewing instructions, searching existing data sources, gathering and maintaining the data needed, and completing and reviewing the collection of information. Send comments regarding this burden estimate or any other aspect of this collection of information, including suggestions for reducing this burden, to Washington Headquarters Services, Directorate for Information Operations and Reports, 1215 Jefferson Davis Highway, Suite 1204, Arlington, VA 22202-4302, and to the Office of Management and Budget, Paperwork Reduction Project (0704-0188), Washington, DC 20503.

1. AGENCY USE ONLY (Leave blank)	2. REPORT DATE 5/9/96	3. REPORT TYPE AND DATES COVERED Final Technical Report
----------------------------------	--------------------------	--

4. TITLE AND SUBTITLE <i>Investigation of sediment dynamics in the nearshore environment.</i>	5. FUNDING NUMBERS N00014-90-J-1189
--	--

6. AUTHOR(S) Richard W. Sternberg	
--------------------------------------	--

7. PERFORMING ORGANIZATION NAME(S) AND ADDRESS(ES) University of Washington School of Oceanography Box 357940 Seattle, WA 98195-7940	8. PERFORMING ORGANIZATION REPORT NUMBER
--	--

9. SPONSORING/MONITORING AGENCY NAME(S) AND ADDRESS(ES) Dept of the Navy Office of the Chief of Naval Research 800 N Quincy St, Code 321CD Arlington, VA 22217-5660	10. SPONSORING/MONITORING AGENCY REPORT NUMBER
---	--

11. SUPPLEMENTARY NOTES

12.a. DISTRIBUTION/AVAILABILITY STATEMENT DISTRIBUTION STATEMENT A Approved for public release Distribution Unlimited	CODE 19970717 078
---	-----------------------------

13. ABSTRACT (Maximum 200 words)

Two major research activities were carried out during this grant period. The first was participation in the DUCK94 field experiment to investigate nearbed fluid motions and resulting sediment resuspension in the surf zone. Data were collected over two three-week periods, in August and October 1994, and included concurrent measurements of velocity and suspended sediment profiles at three cross-shore locations and under a variety of wave and current conditions.

The second activity was participation in a controlled wave basin experiment to investigate turbulence generated under breaking waves (galley proof attached). Vertical profiles of turbulence intensity were estimated from velocity fluctuations. Beneath broken waves, turbulence intensity was found to be high throughout the water column and to increase both toward the bed (due to boundary shear) and the sea surface (due to wave breaking). In a simple model using eddy viscosity profiles determined from the turbulence intensities, the surface turbulence generated by wave breaking would cause suspended sediments to be distributed higher into the water column than existing models would predict considering turbulence generated only at the bottom boundary. This redistribution of suspended sediment would have a significant impact on sediment flux in the surf zone.

At present we are analyzing the DUCK94 data set in two ways. First, the eddy viscosity profiles from the wave basin experiment are being used to understand observed suspended sediment profiles and particle flux. Second, cross-shore flux divergence of sediment is being used to explain observed changes in the beach profile (i.e., net deposition and erosion).

14. SUBJECT TERMS	15. NUMBER OF PAGES 1
	16. PRICE CODE

17. SECURITY CLASSIFICATION OF REPORT None	18. SECURITY CLASSIFICATION OF THIS PAGE None	19. SECURITY CLASSIFICATION OF ABSTRACT None	20. LIMITATION OF ABSTRACT UL
---	--	---	----------------------------------



DEPARTMENT OF THE NAVY
OFFICE OF NAVAL RESEARCH
SEATTLE REGIONAL OFFICE
1107 NE 45TH STREET, SUITE 350
SEATTLE WA 98105-4631

IN REPLY REFER TO:

4330
ONR 247
11 Jul 97

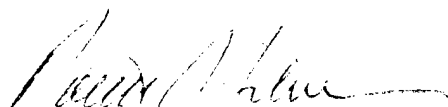
From: Director, Office of Naval Research, Seattle Regional Office, 1107 NE 45th St., Suite 350,
Seattle, WA 98105

To: Defense Technical Center, Attn: P. Mawby, 8725 John J. Kingman Rd., Suite 0944,
Ft. Belvoir, VA 22060-6218

Subj: RETURNED GRANTEE/CONTRACTOR TECHNICAL REPORTS

1. This confirms our conversations of 27 Feb 97 and 11 Jul 97. Enclosed are a number of technical reports which were returned to our agency for lack of clear distribution availability statement. This confirms that all reports are unclassified and are "APPROVED FOR PUBLIC RELEASE" with no restrictions.

2. Please contact me if you require additional information. My e-mail is silverr@onr.navy.mil and my phone is (206) 625-3196.


ROBERT J. SILVERMAN

Estimation of Turbulence-Dissipation Rates and Gas-Transfer Velocities in a Surf Pool: Analysis of the Results from WABEX-93

A. S. Ogston ¹, C. R. Sherwood ², and W. E. Asher ²

¹School of Oceanography University of Washington
Seattle Washington 98195, U.S.A.

² Pacific Northwest Laboratory/Marine Sciences Laboratory
1529 W. Sequim Bay Road, Sequim Washington 98382, U.S.A.

Abstract

As part of the 1993 Wave Basin Experiment (WABEX-93), water velocities and gas fluxes were measured in a surf pool in Irvine, California, under plunging and spilling waves with heights up to 1.2 m. Vertical profiles of turbulence-dissipation rates were estimated from the velocity measurements made with an Acoustic Doppler Velocimeter (ADV). The ADV measured three components of velocity at a sampling rate of 25 Hz. Turbulence-dissipation rates were estimated from the magnitude of the wavenumber spectra of vertical velocity using the universal form for the inertial subrange. Dissipation rates beneath unbroken waves were found to be low in magnitude and uniform in the vertical. Beneath broken waves, dissipation rates were found to be significantly higher in magnitude throughout the water column and to increase toward the water surface. Near-surface dissipation rates beneath breaking waves were found to follow an exponential dependence on whitecap coverage for all but one wave height condition. This suggests that whitecap coverage can be used to scale increases in dissipation rate for breaking waves. The gas transfer velocity due to turbulence generated by near-surface currents and nonbreaking waves, and the gas transfer velocity due to turbulence generated by breaking waves have been estimated from their respective dissipation rates. These transfer velocities have been used with the bubble-mediated transfer velocity to predict the total gas transfer velocity in the surf pool. Predicted gas transfer velocities agree well with measured gas transfer velocities.

1 Introduction

The flux of gases to or from bodies of water can be estimated as the product of the air-water concentration difference, ΔC , of a gas and its transfer velocity, k_L . Because of the difficulties associated with direct oceanic measurements of k_L , it is often calculated from parameterizations derived empirically from wind speed. High surface winds generate surface currents and breaking waves, which generate bubbles and affect mixing. As part of an experiment designed to help develop a method for estimating k_L at high wind speed, gas fluxes and turbulence were measured in a large outdoor

surf pool. A more complete description of the experiment and the gas-flux measurements can be found in Asher et al. [1995] and Wanninkhof et al. [1995].

Results from the gas-exchange measurements suggest that k_L can be partitioned into a component due to near-surface turbulence generated by currents and nonbreaking waves (k_M), one due to turbulence generated by breaking waves (k_T), and one due to bubble-mediated transfer (k_B). For gas evasion with ΔC much less than zero, k_L can be written in terms of the fractional area of whitecap coverage, W_C , as

$$k_L = (k_M + W_C(k_T - k_M)) + W_C k_b \quad (1)$$

Asher et al. [1995] showed that (1) could be applied to gas transfer measured in the surf pool using an explicit functional form for k_B developed using data collected in a whitecap simulation tank. Although (1) provided reasonable estimates of k_L in the surf pool, it was observed to systematically underpredict k_L when W_C was small. Asher et al. [1995] hypothesized that this discrepancy was caused by incorrectly parameterizing the dependence of k_M and k_T on W_C .

Equation 1 was derived by assuming that k_M and k_T were constant and not functions of W_C . Because k_M and k_T are determined by the vertical structure and intensity of the near-surface aqueous-phase turbulence, they are constant only if the turbulence in the surf pool is constant as W_C changes. However, it is reasonable to expect that the turbulence associated with breaking waves increases with wave height and that the background turbulence levels in the surf pool will increase with increasing wave energy. The present study confirms that the turbulence-dissipation rate increases with wave height. Furthermore, the increase in dissipation rate can be scaled using the whitecap coverage of the breaking waves, and inclusion of turbulence-dissipation rates in estimating k_M and k_T improves the ability of (1) to predict gas transfer velocities.

2 Experiment

As part of the 1993 Wave Basin Experiment (WABEX-93), estimates of turbulence-dissipation rates were made in the Hurricane Harbor surf pool at Wild Rivers Waterpark in Irvine, California, under breaking waves with heights up to 1.2 m (see Asher et al. [1995] for details of the surf pool and wave generation). The objective of the measurements described here was to obtain velocity profiles and pressure measurements at multiple locations in the surf pool with resolution sufficient to estimate profiles of turbulence-dissipation rate.

Turbulence-dissipation rates were estimated from velocity measurements made with a SonTek acoustic-doppler velocimeter (ADV). The ADV measured

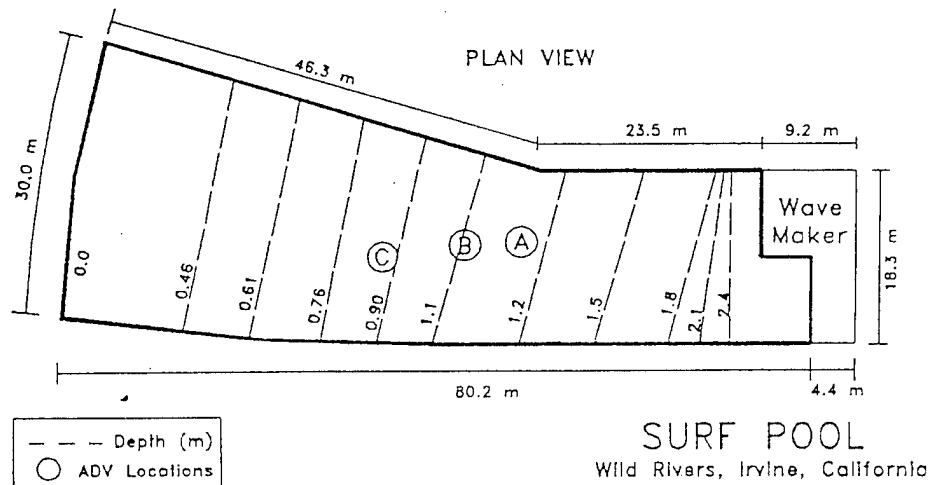


Figure 1: Plan view of the surf pool at Wild Rivers Waterpark in Irvine, California, showing the three ADV measurement locations.

three components of velocity in a 0.5-cm^3 sampling volume located 10 cm below the probe, minimizing the effect of the sensor on the flow field. Measurements were recorded at 25 Hz for runs lasting approximately 300 s (70-100 waves). Because the wave field was highly repeatable, profiles were made by compositing data from three to seven runs, each with the instrument mounted at the same horizontal location but at a different elevation. Profiles were obtained at three locations across the surf zone under spilling and plunging waves generated at four energy levels by the wavemaker, with nominal unbroken wave heights of 0.3, 0.6, 0.9 and 1.2 m. Figure 1 is a schematic drawing of Hurricane Harbor showing the three ADV measurement locations, denoted A, B, and C. Simultaneous measurements of pressure were made with a precision strain-gage located on the bottom directly beneath the ADV. When ADV measurements were made very close (<15 cm) to the bottom the pressure transducer was located ~ 30 cm to the side. Video images of the water surface were recorded and later used to determine wave type and breaker location.

3 Data Analysis

Flow beneath waves can be separated into three components: mean, periodic (wave), and fluctuating (turbulence) components. The objective of the data analysis was to quantify the turbulence component. Several approaches were considered. In laboratory studies with highly repeatable waves, all velocity deviations from the ensemble-mean wave velocity can be attributed to turbulence (Nadaoka et al. [1983]). Although waves in the surf pool ap-

peared quite regular, the detailed pressure measurements showed wave-to-wave variations in pressure. Irregularity in the wave field was most likely caused by the combined effects of variability in the wavemaker, seiching of the pool, reflected waves, and episodic outbreaks of a rip current. Estimates of turbulence based on deviations from the ensemble-mean velocity were precluded because they would overestimate turbulence by including non-turbulent, pressure-induced fluctuations. An alternative approach for extracting turbulence from velocity records involves the portion of the records associated with wave-induced variations of the water-surface (Kitaigorodskii et al. [1983], Agrawal and Aubrey [1992]). This frequency-domain method assumes that velocity variations that are coherent with pressure fluctuations are caused by two-dimensional progressive waves, and that noncoherent velocity fluctuations can be attributed to turbulence. However, the technique is prone to error if waves have directional spread (Herbers and Guza [1993]). We instead used the inertial dissipation method of George et al. [1994], modified to take advantage of the nearly regular wave field and the measurement capabilities of the ADV.

3.1 Data Processing

One advantage of the ADV was its ability to rapidly re-establish good velocity measurements after the loss of acoustic signals in bubble plumes or during subaerial exposure in the trough of a wave. Initial processing identified and rejected data from times when the ADV was exposed or large amounts of bubbles were present. A preliminary criterion for rejection was based on the correlation coefficient between the transmitted acoustic signal and the received backscattered signal. Data-rejection rates increased from near zero at depth to as much as 37% near the surface under larger waves. Acceptable data for 70 to 100 successive waves were phase aligned using the peak in the cross covariance of the slope of the pressure signal, and ensemble means and standard deviations for three velocity components and pressure were estimated (Figure 2). An iterative check on data was then performed: data were rejected if the velocity magnitude exceeded 3.7 standard deviations about the ensemble mean at each phase in the wave, and ensemble statistics were recalculated. Finally, mean and root-mean-square (RMS) velocities were determined for acceptable data from each data run.

3.2 Estimates of Dissipation Rates

In steady flow with isotropic, fully-developed turbulence, kinetic energy is transferred from the mean flow to large eddies, then to small eddies, and is finally dissipated by viscosity. Under these conditions, the turbulence-dissipation rate can be estimated by the magnitude of the wavenumber spectra in the inertial subrange, which takes the form:

$$E(\kappa) = \alpha \varepsilon^{2/3} \kappa^{-5/3} \quad (2)$$

where κ is wavenumber, $E(\kappa)$ is wavenumber spectral density, ε is the turbulence dissipation rate, and α is the Kolmogorov constant. The inertial subrange extends from large eddies, the scale of which is typically determined by physical dimensions of the flow (e. g., depth) to the Kolmogorov microscale, which is determined by kinematic viscosity and dissipation rate.

Estimates of dissipation rate were made for the surf pool data using (2), and assume that the turbulence was fully developed and isotropic. The vertical component of the ADV velocity signal was used to calculate dissipation rates because it had the highest signal-to-noise ratio of the three components. Spectral estimates were obtained using a windowing and ensemble-averaging (Welch) method. Because data were removed during initial processing, the spectra for each windowed time series was computed using a method appropriate for irregularly spaced data (Press et al. [1992]). Entire data windows were omitted if more than 50% of the data points were missing. Spectral estimates were obtained by first detrending the data by subtracting out the ensemble-mean periodic (wave) velocity component, then computing spectra on a windowed data segment extending over three successive waves, and finally ensemble-averaging the spectra. Windowed segments were overlapped 67%. This procedure yielded spectral estimates with resolved bandwidths of 0.16 Hz and 156 degrees of freedom for typical time series containing 80 waves.

The time-series data at a fixed point were used to estimate the energy-density spectrum as a function of frequency, not wavenumber. The frequency spectra were converted to wavenumber spectra using Taylor's hypothesis of frozen turbulence, assuming that the time scale of turbulent fluctuations was long compared with the time scale of the motion advecting the eddy past the sampling point. The RMS orbital velocity was used as the advective velocity for the conversion from measured frequency spectra to wavenumber spectra (Agrawal et al. [1992]). An example of the wavenumber spectra generated from the vertical velocity data is shown in Figure 3.

Turbulence-dissipation rates (ε) were estimated from the magnitude of the wavenumber spectra in the inertial subrange using (2). For each data run, the wavenumber spectra were individually inspected and the magnitude of the spectra in the range over which the theoretical -5/3 slope was found was used to estimate the dissipation rate (typically between radian wavenumbers of 0.4 and 1.5 cm^{-1}).

4 Turbulence Dissipation Results

Profiles of ε beneath plunging waves are shown in Figures 4a and 4b, and beneath spilling waves in 4c. Elevation is normalized by the water depth,

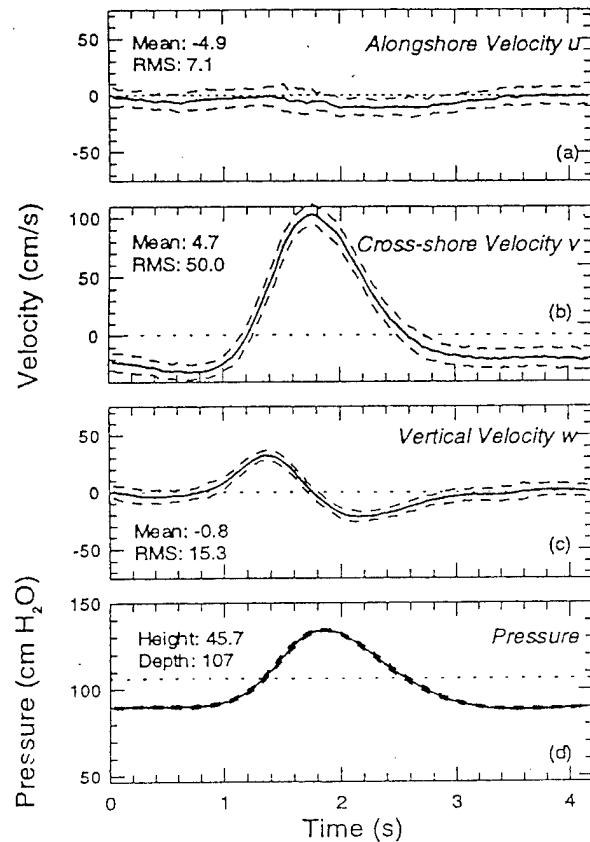


Figure 2: Ensemble-average velocities and pressure under plunging wave of nominal height 0.9 m at location A, 53 cmab: *a* Alongshore velocity. *b* Cross-shore velocity. *c* Vertical velocity. *d* Pressure.

so that a normalized elevation of 1.0 is at the mean water surface. Under unbroken waves, ϵ profiles were generally low in magnitude and vertically uniform. Beneath plunging waves measured at location A (Figure 4a), ϵ was highest near the surface and increased with increasing wave height. Dissipation rates were also seen to increase with increasing wave height throughout the water column.

Profiles of ϵ at location B (Figure 4b) are similar to profiles at location A (Figure 4a), although the mid-water column ϵ are higher at B, and there is at B little difference in ϵ between the 0.9-m and 1.2-m wave conditions. Strong rip currents at B could be responsible for the increase in the ϵ for the mid-water column compared with A. Alternatively, the increased distance from breaking (cross-shore location) at B could have allowed homogenization of turbulence through the water column. Similar values of ϵ for wave heights

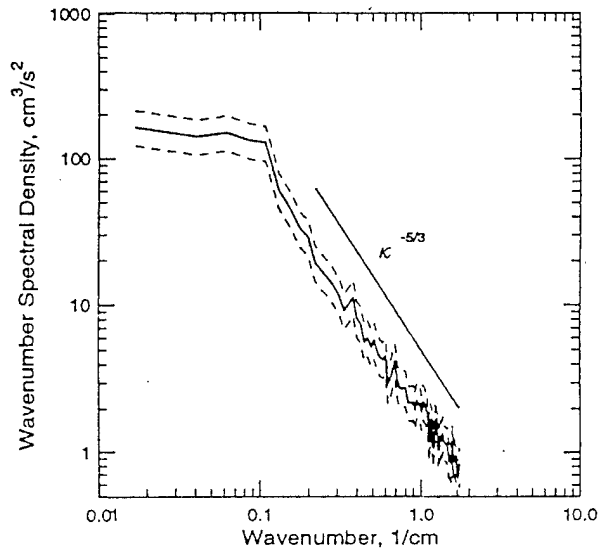


Figure 3: Representative wavenumber spectrum of vertical velocity showing inertial subrange ($\kappa^{-5/3}$ slope) under plunging wave of nominal height 0.9 m at location A, 53 cmab.

of 0.9 m and 1.2 m could indicate a saturation value for ϵ at some distance from the break point. At B, velocity measurements were made very close to the pool bottom, and observed increases in ϵ are likely associated with shear-induced turbulence in the bottom boundary layer (Figure 4b).

Beneath spilling waves at location C (Figure 4c), profiles of ϵ show more variation, possibly because spilling waves were less regular. Like ϵ measured beneath plunging waves at B, ϵ was high in the middle of the water column but, in contrast to measurements of ϵ at B, ϵ measured beneath spilling waves at C did not appear to reach saturation near the surface.

4.1 Characteristic Dissipation Rates

Dissipation rates from two depths were used to characterize turbulence generated by breaking waves (ϵ_T), and background mechanical turbulence generated by currents and nonbreaking waves (ϵ_M). The ϵ_T was taken to be the ϵ interpolated at a normalized elevation of 0.8 for the plunging waves, and 0.65 for the spilling waves (upper limit of measurements). These depths are consistent with the assumption that the dominant length scale for turbulence generated by wave breaking is proportional to the breaking wave amplitude. It was assumed that the characteristic ϵ_T and ϵ_M for gas exchange in the entire surf pool were less than ϵ_T and ϵ_M at location A and greater than ϵ_T and ϵ_M at location B beneath plunging waves, and that the characteristic

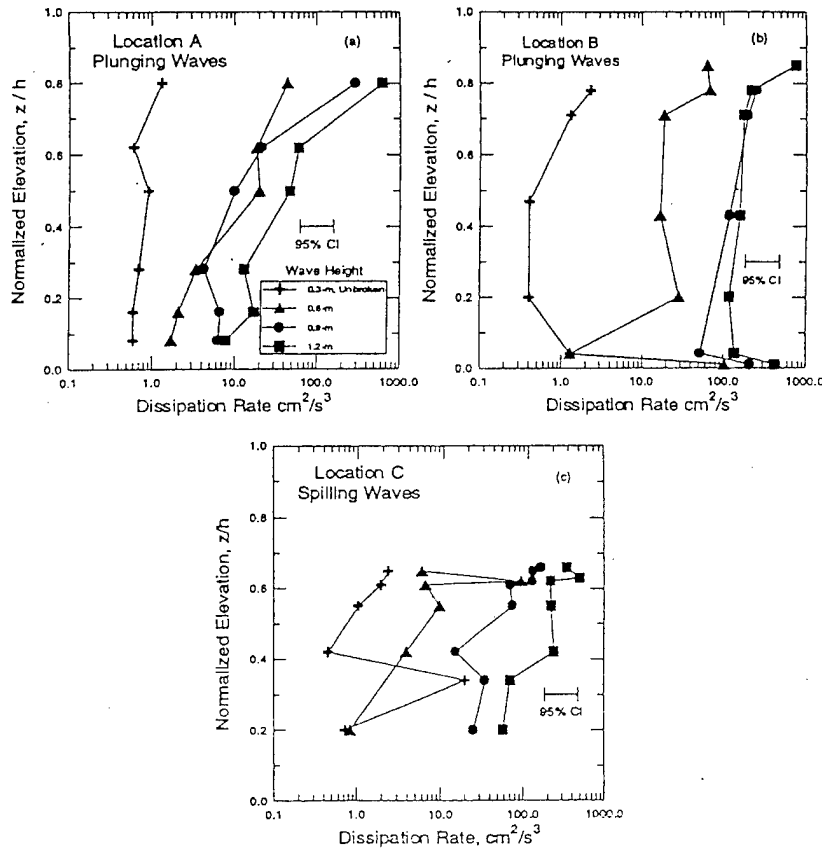


Figure 4: Vertical profiles of turbulence-dissipation rate, ϵ , beneath a plunging waves at location A, b plunging waves at location B, and c spilling waves at location C, of nominal waveheights 0.3, 0.6, 0.9, 1.2 m.

ϵ_T and ϵ_M were approximately equal to ϵ_T and ϵ_M at location C beneath the spilling waves. Values for ϵ_T are listed in Table 1 for the two wave types and four wave heights. The dissipation rate for turbulence generated by non-breaking waves and currents, ϵ_M , was determined at a normalized elevation of 0.2 (Table 1). This level was generally below the region of large gradients in the ϵ profiles. Turbulence generated in the bottom boundary layer was observed below this level (Figure 4b), but does not appear to influence ϵ above normalized elevations of 0.1.

4.2 Dissipation Rates and Whitecap Coverage

The area-weighted fractional coverage of actively breaking waves, W_C , was measured in the pool (Asher et al. [1995]), and values are listed in Table

Table 1: Turbulence-dissipation rates and whitecap coverage

Wave Type	Nominal Height	ϵ_M (cm ² /s ³)	ϵ_T (cm ² /s ³)	W_C (%)
Plunging	1.2 m	75	499	7.15
Plunging	0.9 m	45	299	3.96
Plunging	0.6 m	2	66	2.01
Plunging	0.3 m	0.6	0.8	0.00
Spilling	1.2 m	65	428	2.90
Spilling	0.9 m	21	152	2.51
Spilling	0.6 m	5	6	0.54
Spilling	0.3 m	1	2	0.00

1. Figure 5 is a log-normal plot of ϵ_T versus W_C from the data in Table 1. ϵ for spilling waves at all four heights and ϵ_T for breaking waves with heights of 0.3 m, 0.6 m, and 0.9 m were found to follow the same exponential dependence on W_C . This suggests that W_C can be used to scale increases in ϵ_T caused by breaking waves. It is not clear why ϵ_T for the 1.2-m plunging breaking waves does not follow the same dependence as the other seven wave conditions, but it should be noted that these conditions presented the most difficult data-analysis problems, and many data points during the times of high velocities were eliminated. As a result, maximum dissipation rates could have been underestimated.

5 Parameterization of Gas Transfer Velocities

Lamont and Scott [1970] showed that for gas exchange across an unbroken water surface, k_L could be estimated using ϵ . Using their relation, k_M and k_T can be written as

$$k_X = BSc^{-1/2}(\epsilon_X\nu)^{1/4} \quad (X = M, T) \quad (3)$$

where B is a dimensionless constant, Sc is the Schmidt number of the gas (equal to the ratio of kinematic viscosity to molecular diffusivity), ν is the kinematic viscosity of water, and ϵ_M and ϵ_T are the dissipation rates of the wave-current-generated turbulence and the breaking-generated turbulence, respectively. In support of (3), Asher and Pankow [1986] found that k_L for transfer of carbon dioxide (CO₂) through a cleaned water surface scaled linearly with $\epsilon^{1/4}$. They also found that B was equal to 0.65.

Asher et al. [1995] measured k_L for CO₂, helium (He), nitrous oxide (N₂O), and sulfur hexafluoride (SF₆) as a function of W_C in the surf pool. They developed an empirical parameterization of k_L using (1) by assuming k_M and k_T were constant with increasing W_C and taking $k_B = b_1\alpha^{-0.043}Sc^{-0.35}$. As

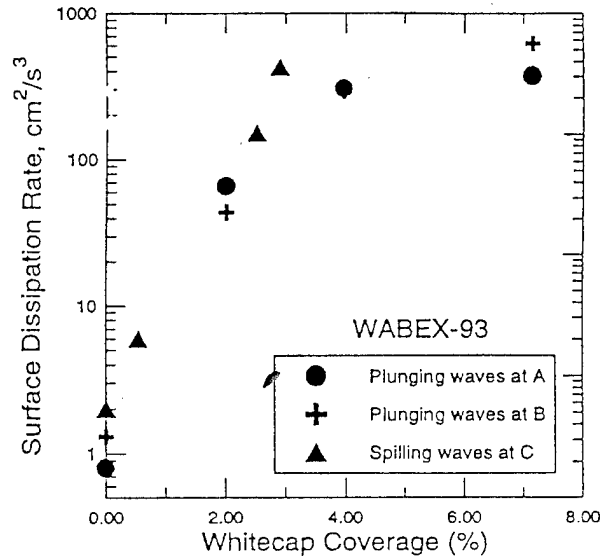


Figure 5: Whitecap coverage, W_C , versus surface turbulence-dissipation rate, ϵ_T , for plunging waves at locations A and B and spilling waves at location C.

can be seen in Figure 5 however, ϵ_M and ϵ_T were not constant with increasing W_C , and (3) shows k_M and k_T will also increase. Therefore, it is not surprising that Asher et al. [1995] found that parameterizing k_L using (1) and assuming that k_M and k_T were constant was unsatisfactory.

The dissipation rates listed in Table 1 were used to calculate k_M and k_T using (3) and assuming B would be a constant fit by the data. These transfer velocities were substituted into (1) to account for the effect of the increase in turbulence with increasing W_C . Written explicitly, k_L in the wave basin can be parameterized as

$$k_L = B(\epsilon_M \nu)^{1/4} + W_C \left((\epsilon_T \nu)^{1/4} - (\epsilon_M \nu)^{1/4} \right) S_C^{1/2} + b_1 W_C \alpha^{-0.043} S_C^{-0.35} \quad (4)$$

The resulting model was then fit using least-squares linear regression to the measured k_L data from Asher et al. [1995] to determine the coefficients b_1 and B in (4). This fit results in $B = 0.58$ and $b_1 = 6.30 \text{ m s}^{-1}$ with a coefficient of determination of 0.84. The value of B found for the WABEX-93 data is in good agreement with that determined by Asher and Pankow [1986].

Figure 6 shows the result of fitting (4) to the surf pool data by plotting k_L for CO_2 , He, N_2O , and SF_6 calculated using (4) versus the experimentally determined value. There is excellent agreement between the calculated and measured k_L values. Asher et al. [1995] found a reduced chi-squared (χ^2) of

192 for the constant k_M and k_T parameterization. The χ^2 for the data in Figure 6 was 70, which shows that including the effects of increasing turbulence with increasing W_C improves the predictive accuracy of a parameterization based on (1).

The parameterization given in (4) can also be used to estimate the fraction of k_L that is due to turbulence and the fraction of k_L that results from bubble-mediated processes. For SF₆ for a 0.9-m spilling wave, turbulence processes accounted for 38% of the total transfer velocity and bubble processes were 62% of the total. In contrast, the turbulence fraction for CO₂ under the same conditions was 46% and the bubble fraction was 54%. The decreased importance of bubble-mediated transfer for CO₂ compared with SF₆ agrees with the model predictions of Memery and Merlivat [1985]. Their results indicated that k_B for a soluble gas such as CO₂ would be less than k_B for an insoluble gas like SF₆.

6 Conclusion

Turbulence dissipation rates were found to increase with increasing wave height for spilling and plunging waves. The surface dissipation rates scaled as an exponential function of whitecap coverage for spilling waves with nominal heights of 0.3 m, 0.6 m, 0.9 m, and 1.2 m and for plunging waves with nominal heights of 0.3 m, 0.6 m and 0.9 m. For reasons that are not clear at present, the surface dissipation rate for plunging waves with a height of 1.2 m did not follow this exponential scaling.

Asher et al. [1995] found that parameterizing k_L for CO₂, He, N₂O, and SF₆ assuming k_M and k_T were constants did not provide a satisfactory fit with the measured surf pool data ($\chi^2 = 192$). Substitution of the direct estimates of k_M and k_T from (3) and dissipation rates estimated from the surf pool measurements improved the agreement between measured and predicted k_L values ($\chi^2 = 70$).

In the surf pool, increases in W_C were caused by increases in height of the breaking wave. It could be expected that a similar process occurs under oceanic conditions, where increasing wind speed leads to larger wave size and higher whitecap coverage. The success of the approach described here suggests that successful application of (1) to ocean conditions will require knowledge of k_B and the dependence of k_M and k_T on wind speed. Although this complicates the parameterization of k_L in the ocean, it will provide an accurate estimation of the effect of the turbulence and bubbles generated by breaking waves on air-sea gas fluxes.

Acknowledgements

This research was supported by the U.S. Department of Energy (DOE), Office of Health and Environmental Research, Environmental Sciences Division under Contract DE-AC06-76RLO 1830. Pacific Northwest Laboratory (PNL) is

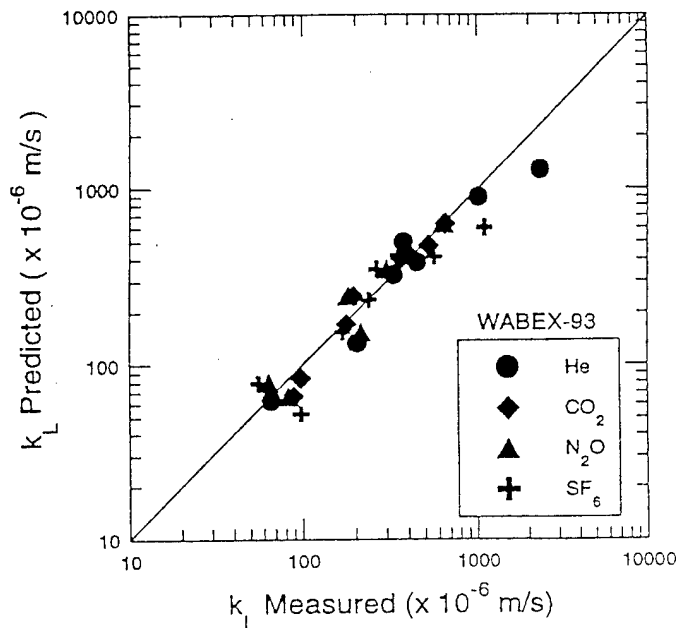


Figure 6: Measured versus predicted total gas transfer velocity, k_L , for He, CO₂, N₂O, and SF₆.

operated for DOE by Battelle Memorial Institute. We appreciate the assistance of Atle Lohrmann of SonTek, Inc., who provided an early model of the ADV. Andrea Ogston is a graduate fellow at PNL under the Associated Western Universities Northwest program and has also been supported by the Office of Naval Research.

References

- Agrawal, Y. C., and D. G. Aubrey, [1992] Velocity observations above a rippled bed using laser Doppler velocimetry, *J. Geophys. Res.*, 97, 20249-20259.
- Agrawal, Y. C., E. A. Terray, M. A. Donelan, P. A. Hwang, A. J. W. III, W. M. Drennan, K. K. Kahma, and S. A. Kitaigorodskii, [1992] Enhanced dissipation of kinetic energy beneath surface waves, *Nature*, 359, 219-220.
- Asher, W. E., and J. F. Pankow, [1986] The interaction of mechanically generated turbulence and interfacial films with a liquid phase controlled gas/liquid transport process, *Tellus*, 38B, 305-318.
- Asher, W., L. Karle, B. Higgins, P. Farley, C. Sherwood, W. Gardiner, R. Wanninkhof, H. Chen, T. Lantry, M. Steckley, E. Monahan, Q. Wang, and P. Smith, [1995] Measurement of gas transfer, whitecap coverage, and brightness temperature in a surf pool: an overview of WABEX-93, in *Proceedings of the Third International Symposium on Air-Water Gas Transfer*, edited by B. Jähne and E. C. Monahan, AEON Verlag, Heidelberg, Germany, July 24-27.

- George, R., R. E. Flick, and R. T. Guza, [1994] Observations of turbulence in the surf zone, *J. Geophys. Res.*, 99, 801-810.
- Herbers, T. H. C., and R. T. Guza, [1993] Comment on "Velocity observations above a rippled bed using laser doppler velocimetry" by Y. C. Agrawal and D. G. Aubrey, *J. Geophys. Res.*, 98, 20331-20333.
- Kitaigorodskii, S. A., M. A. Donelan, J. L. Lumley, and E. A. Terray, [1983] Wave-turbulence interactions in the upper ocean. Part II: Statistical characteristics of wave and turbulent components of the random velocity field in the marine surface layer, *J. Phys. Oceanogr.*, 13, 1988-1999.
- Lamont, J. C., and D. S. Scott, [1970] An eddy cell model of mass transfer into the surface of a turbulent liquid, *A.I.Ch.E.J.*, 16, 513-519.
- Memery, L., and L. Merlivat, [1985] Modeling of the gas flux through bubbles at the air-water interface, *Tellus*, 37B, 272-285.
- Nadaoka, K., M. Hino, and Y. Koyano, [1989] Structure of the turbulent flow field under breaking waves in the surf zone, *J. Fluid Mech.*, 204, 359-387.
- Press, W. H., S. A. Teukolsky, W. T. Vetterling, and B. P. Flannery, [1992] Numerical Recipes in FORTRAN: the Art of Scientific Computing, *Cambridge University Press*, New York, 963 pp..
- Wanninkhof, R., W. E. Asher, and E. C. Monahan, [1995] The influence of bubbles on air-water gas exchange: Results from gas transfer experiments during WABEX-93, in Proceedings of the Third International Symposium on Air-Water Gas Transfer, edited by B. Jähne and E. C. Monahan, AEON Verlag, Hanau, Germany, July 24-27, 1995.